Alternating field demagnetization, single-domain-like memory, and the Lowrie-Fuller test of multidomain magnetite grains (0.6–356 μm)

David J. Dunlop, Song Xu,[1] and Franz Heider[2]
Geophysics, Physics Department, University of Toronto, Toronto, Ontario, Canada

Received 2 February 2004; revised 23 April 2004; accepted 3 May 2004; published 3 July 2004.

[1] A fundamental question in paleomagnetism is how magnetite grains much larger than single-domain size preserve stable remanence over millions of years. In an effort to answer this question we measured alternating field (AF) demagnetization of thermoremanent magnetization (TRM) and saturation isothermal remanent magnetization (SIRM) before and after low-temperature demagnetization (LTD). LTD (zero-field cycling through 120 K) unpins or nucleates domain walls, reducing the remanence of multidomain grains. We used two sets of sized crushed magnetites (0.6, 1, 3, 6, 9, 14, 20, 110, and 135 μm), one set unannealed and the other annealed, and a set of hydrothermally grown magnetites (0.8, 6.3, 25, 64, 94, and 356 μm). For all sizes, TRM and SIRM memories after LTD are much harder to AF demagnetize than the original remanences. AF demagnetization curves after LTD are flat for the first ∼10 mT. Such initial plateaus are one hallmark of single-domain behavior. In high-stress unannealed grains, after-LTD response depends on grain size, larger grains demagnetizing more easily than smaller ones. In low-stress annealed and hydrothermal magnetites, after-LTD response is almost independent of grain size over nearly 3 decades in grain size. This size-independent behavior could be due to grains in metastable single-domain states in the smaller-sized samples, but in >100 μm grains, there must be a source of single-domain-like AF behavior within the multidomain grains themselves. We propose an ad hoc model in which LTD triggers domain wall unpinning and nucleation events up to a coercivity threshold, producing the observed initial plateaus in AF demagnetization curves of TRM and SIRM memories. The size-independent demagnetization behavior of memory in hydrothermal and annealed magnetites is ascribed to nucleation events above the threshold level, and the additional size-dependent AF demagnetization of memory in high-stress unannealed grains is explained by wall unpinning from strong stress centers. In both cases the AF properties merely mimic single-domain behavior. Although LTD memory has single-domain-like AF curves and erased remanence has multidomain-like curves in grains of all sizes, the *Lowrie and Fuller* [1971] test still works for the annealed samples. For memory, erased fraction and pre-LTD remanence alike, TRM is more stable than SIRM in fine grains (1 μm), less stable in large grains (135 μm), and of comparable stability in medium-size grains (9 and 20 μm). *INDEX TERMS:* 1512 Geomagnetism and Paleomagnetism: Environmental magnetism; 1521 Geomagnetism and Paleomagnetism: Paleointensity; 1533 Geomagnetism and Paleomagnetism: Remagnetization; 1540 Geomagnetism and Paleomagnetism: Rock and mineral magnetism; *KEYWORDS:* alternating field demagnetization, low-temperature memory, multidomain magnetite

Citation: Dunlop, D. J., S. Xu, and F. Heider (2004), Alternating field demagnetization, single-domain-like memory, and the Lowrie-Fuller test of multidomain magnetite grains (0.6–356 μm), *J. Geophys. Res.*, *109*, B07102, doi:10.1029/2004JB003006.

1. Introduction

[2] Most magnetite grains in rocks are larger than the critical single-domain (SD) size d_0 = 0.07–0.08 μm [*Enkin and Williams*, 1994; *Newell and Merrill*, 1999]. They nevertheless often record paleomagnetic information that has survived unchanged for millions of years and is resistant to laboratory demagnetization by alternating fields (AF) or temperature. Such high time stability and resistance to laboratory cleaning are not expected for multidomain (MD) grains containing rather easily moved domain walls subject to internal self-demagnetizing fields.

[3] To account for the stable paleomagnetic properties of small multidomain grains, *Verhoogen* [1959] proposed that

[1]Now at JDL Digital Systems, Seattle, Washington, USA.
[2]Now at Physical Failure Analysis, Infineon Technologies, Villach, Austria.

0148-0227/04/2004JB003006$09.00

regions surrounding crystal dislocations could behave as SD-like magnetic moments. *Stacey* [1962, 1963] suggested other microscopic mechanisms and coined the term pseudo-single-domain (PSD) to describe them. On the basis of measurements of thermoremanent magnetization (TRM) and hysteresis of sized magnetites [*Parry*, 1965], *Stacey and Banerjee* [1974] suggested that PSD moments were prominent in grain sizes from d_0 to 10–20 μm, and this has come to be known as the PSD range of magnetite.

[4] Over the years the term PSD has been used to describe a variety of experimental properties from paleomagnetic time-temperature stability [*Dunlop et al.*, 1997] to TRM and anhysteretic remanent magnetization (ARM) size and field dependences [*Dunlop and Argyle*, 1997] to laboratory hysteresis and AF behavior transitional between SD and MD [e.g., *Day et al.*, 1977]. PSD has also been applied to theoretical models ranging from domain wall moments [*Dunlop*, 1977] to metastable local-energy-minimum states [*Moon and Merrill*, 1984, 1985] to vortex and other transitional micromagnetic structures [e.g., *Williams and Dunlop*, 1995] and most recently to net moments in irregularly shaped grains [*Fabian and Hubert*, 1999]. Connections among the various phenomena remain speculative. Only the existence of metastable SD grains [*Halgedahl and Fuller*, 1980, 1983] has been demonstrated beyond doubt.

[5] In this paper, we focus on experimental AF demagnetization of TRM, ARM, and saturation isothermal remanent magnetization (SIRM) in magnetites spanning a very broad size range from close to d_0 to large MD crystals hundreds of micrometers in diameter. As a criterion of SD behavior we use an initial flat portion of the AF demagnetization curve from 0 to ∼10 mT. This initial plateau occurs because SD grains have a minimum coercivity due to magnetocrystalline anisotropy K_1 of 10–15 mT [*Dunlop and Özdemir*, 1997, chapter 11]. Below this threshold field, AFs have no effect. MD grains have no such threshold or initial plateau. The internal self-demagnetizing field H_d drives domain walls from the earliest stages of AF cleaning, and the AF curves are of exponential form.

[6] In order to isolate the stable fraction of remanence from the general MD response of large grains, we used low-temperature demagnetization (LTD) prior to AF cleaning. In LTD a remanence-carrying sample is cooled below the magnetite isotropic point (T_K = 130 K) and Verwey transition (T_V = 120 K) and rewarmed to room temperature in zero field. Whereas AF cleaning works by applying a field exceeding the microcoercivity H_c, LTD effectively reduces H_c to zero [*Merrill*, 1970].

[7] Microcoercivity is the field needed to rotate an SD moment, to unpin a domain wall from a stress center in an MD grain, or to nucleate a wall in either an SD or MD grain. LTD is most effective in unpinning domain walls because when $K_1 \rightarrow 0$ at T_K, all walls increase in width and escape from the localized stress fields of dislocations [*Xu and Merrill*, 1989]. LTD should also promote nucleation because the main opposition to reverse nuclei of magnetization is magnetocrystalline lattice coupling. LTD is less effective in unpinning SD moments because shape anisotropy provides an additional barrier to rotation. Therefore LTD tends to greatly reduce the remanence of MD grains, while having much less effect on SD moments [*Kobayashi and Fuller*, 1968].

[8] In previous studies of AF demagnetization before and after LTD, *Dunlop and Argyle* [1991] measured TRM, ARM, and SIRM of magnetites just above SD size (0.215–0.54 μm), *Özdemir and Dunlop* [1998] examined TRM and SIRM of a millimeter-size crystal, and *Muxworthy and McClelland* [2000] reported results for TRM, ARM, and SIRM of 3.0 μm hydrothermal and 190 μm natural crystals. In each case the LTD memory displayed an SD-like region of little or no demagnetization at low AFs. On the other hand, *McClelland and Shcherbakov* [1995] and *McClelland et al.* [1996] have argued that AF response is part of a larger set of properties, most logically explained by metastable states of truly MD grains. The connection between an initial AF plateau and the nucleation or destruction of walls in passing from one metastable state to another was not spelled out.

[9] One major difference between our study and previous ones is that we examine systematically an extremely broad grain size range, from 0.6 μm to 356 μm, spanning previous data gaps. We also investigate the role of internal stress, which is responsible for domain wall pinning by comparing the AF response of crushed grains with large dislocation densities to the response of much less stressed grains, either annealed or produced hydrothermally.

2. Samples and Experiments

[10] Two sets of samples were prepared by hand-crushing large natural crystals of magnetite from Bancroft, Ontario, with a mortar and pestle, taking care to avoid heating that could promote oxidation. The material was separated using sieves into two coarse fractions (125–150 μm with mean size ∼135 μm and 100–125 μm with mean size ∼110 μm) and, using a Bahco centrifugal dust analyzer, into seven fine fractions with mean sizes of 20, 14, 9, 6, 3, 1, and 0.6 μm.

[11] SIRM produced at low temperature (20 K) and warmed in zero field decreased to almost zero at the magnetite Verwey transition for all fractions. Measurements were made every 2 K with an MPMS-2 SQUID magnetometer. T_V was 110–115 K, and the transition was sharp. Using a Kappa bridge, low field susceptibility χ was monitored continuously during warming to and cooling from 700°C in air; χ dropped to near zero just below the magnetite Curie point of 580°C in all samples (Figure 1). The finest grains showed a small signal due to hematite. Their cooling curves were lower than the heating curves, showing that oxidation occurred during heating above 580°C and not during preparation of the magnetite powders. The shapes of the $\chi-T$ curves changed from being temperature-independent (typical MD controlled by self-demagnetization) for the largest grains (Figure 1) to being gentle ramps with a Hopkinson peak for the finest grains.

[12] The remaining material was separated into two lots. One set of nine powders was left in as-prepared condition, while the other set was annealed under vacuum for several hours at 650°–700°C to reduce internal stress as much as possible. The annealed and unannealed powders were dispersed in CaF_2 to a concentration of about 1% by weight and were packed firmly into individual quartz capsules with quartz wool. Following pump down to a hard vacuum (about 1 day), the capsules were sealed off.

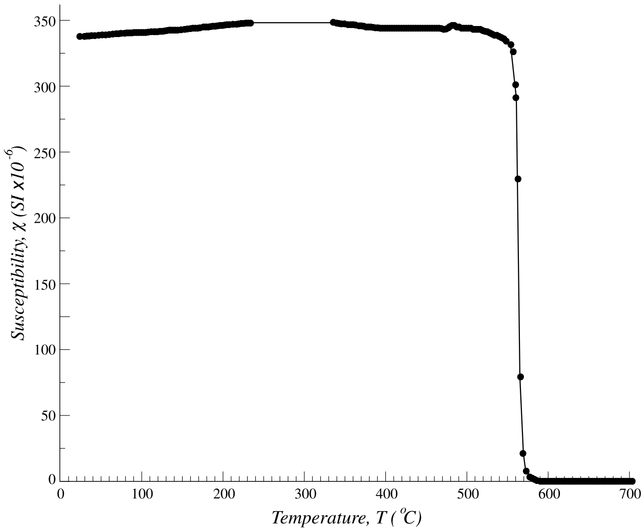

Figure 1. Susceptibility-temperature curve for the 135 μm sample, showing the Curie point of magnetite.

[13] As a third set of samples we used six hydrothermally grown magnetites with mean grain sizes of 0.8, 6.3, 25, 64, 94, and 356 μm. The preparation of these samples was described in detail by *Heider and Bryndzia* [1987]. Their magnetic properties were reported by *Heider et al.* [1987], who established that the levels of internal stress, as measured by dislocation densities, are very low. Low-temperature demagnetization of these and other similar magnetites was carried out by *Heider et al.* [1992], who found that the memory fraction that remains after LTD depends as much on stress and irregularities in the surfaces of grains as it does on grain diameter. Among the larger crystals we chose the most nearly perfect ones for the present study, which greatly augments the AF demagnetization results reported by *Heider et al.* [1992].

[14] We produced and demagnetized in succession TRM, ARM, and SIRM. TRM was produced by cooling each sample from above 600°C to 20°C in a field of 0.1 mT. This TRM was demagnetized in steps to 100 mT using a Schonstedt AF demagnetizer. TRM was again produced and was cycled in zero field to 77 K and back to room temperature using a small dewar inside a five-layer high-permeability mu-metal shield. The TRM memory after LTD was then AF demagnetized. ARM was produced by a steady field of 0.1 mT superimposed on a decaying AF of initial amplitude of 100 mT. The ARM was demagnetized in steps after suppressing the field in the DC coil. ARM was again produced and cycled to 77 K in zero field, and the ARM memory was AF demagnetized. Finally, SIRM produced by the 1-T field of an electromagnet was AF demagnetized. A fresh SIRM was treated by LTD, and the SIRM memory was AF demagnetized in its turn.

3. Experimental Results

3.1. AF Demagnetization Curves Before and After LTD

[15] AF demagnetization curves of TRM for the nine crushed and annealed magnetites are compared in Figure 2. The two largest grain-size samples, 110 and 135 μm, have AF curves that approach MD exponential form [*Xu and Dunlop*, 1993], but not even the finest grains, 0.6 μm, have a truly SD-like curve. The shape is inflected, but demagnetization begins at the lowest AFs. There is no initial SD plateau.

[16] The shapes of the AF demagnetization curves change monotonically with grain size between the limiting curves of the smallest and largest magnetites. Within this set of magnetites at least, AF curve shape is diagnostic of grain size and/or domain state.

[17] AF demagnetization curves of TRM, ARM, and SIRM for the 1 μm sample are compared in Figure 3a. Weak field TRM and ARM are considerably more resistant to AF demagnetization than strong field SIRM, an SD-type result of the *Lowrie and Fuller* [1971] test. For the first ∼10 mT the ARM demagnetizes somewhat more quickly than the TRM, at first almost as rapidly as SIRM. This small initial difference in behavior between ARM and TRM has been noted previously [*Dunlop and Argyle*, 1991, 1997].

[18] TRM, ARM, and SIRM memories after LTD are 67%, 64%, and 52% of the initial remanences, respectively. The memory remanences demagnetize in a distinctive way. Very little demagnetization occurs in the first 10 mT, and the curves are perfectly flat from 0 to 5 mT. As well as this initial plateau, the curves are now strongly inflected in typical SD fashion. The inflection points are around 25–30 mT, just below the field level at which the memory and uncleaned remanence curves merge.

[19] Some similarities and some differences appear in the weak field TRM and SIRM demagnetization curves for the 135 μm sample (Figure 3b). Unlike the finer magnetites, the demagnetization curves of the untreated remanences are quasi-exponential in form, and above 10 mT, SIRM is somewhat more resistant to AF cleaning than weak field TRM, an MD-type result of the Lowrie-Fuller test. However, after LTD both TRM and SIRM memories have

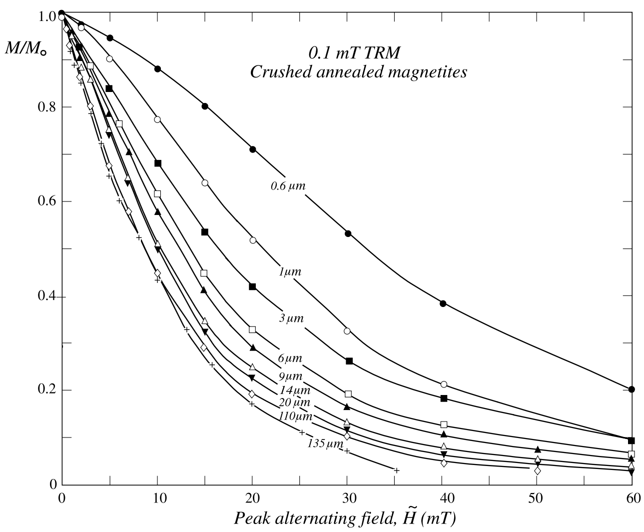

Figure 2. AF demagnetization of weak field TRM for the nine crushed and annealed magnetite samples. Curve shapes and coercivity ranges change dramatically with grain size.

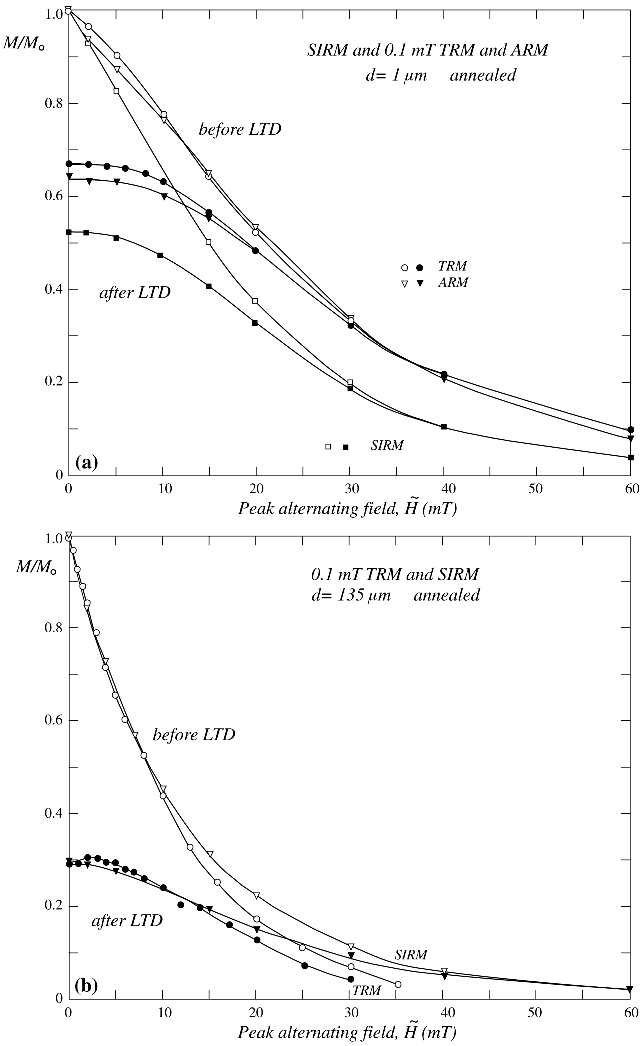

Figure 3. Comparisons of AF demagnetization of SIRM and weak field TRM and ARM. (a) For the annealed 1 μm magnetite sample, LTD prior to AF cleaning removes part of the remanence with H_c < 30 mT and almost all remanence with H_c < 10 mT. (b) For the annealed 135 μm magnetite sample, LTD prior to AF cleaning again removes low-coercivity remanence, producing an initial plateau in the AF curves.

inflected demagnetization curves with initial plateaus, although the memory ratios are about one half those of the 1 μm magnetites.

3.2. AF Decay Curves of LTD Memory and Erased Fractions

[20] The memory is the fraction of remanence that survives LTD, and the memory AF decay curve is directly measured. A decay curve for the fraction erased by LTD is obtained by subtracting the memory decay curve from the pre-LTD total remanence decay curve. In general, we find that the memory decay curves are hard (10–60 mT), are inflected in shape, and have an initial plateau (SD like, as shown in Figures 3a and 3b), while the erased fraction is soft (0–25 mT) and decays exponentially (MD-like behavior).

[21] SIRM results for eight of the nine samples in the unannealed suite of crushed magnetites appear in Figure 4a. The erased fraction has an exponential-like decay curve, except for the two finest magnetites (0.6 and 1 μm), which have slightly inflected curves. The memory decay curves are strongly inflected and SD-like for all grain sizes, the initial plateaus being particularly marked for the finer grain sizes. Within either group of curves, there is a monotonic dependence on grain size, finer grains being harder to demagnetize and coarser grains being softer.

[22] Considering the wide range of shapes within either group of curves in Figure 4a, it is remarkable that the same magnetites, when annealed to reduce internal stress, give entirely different results (Figure 4b). Within both the SIRM memory and erased fraction groups all the decay curves have almost exactly the same shape. The slight grain size dependence of the memory decay curves is very minor compared to that in Figure 4a. Inflections have disappeared from the erased fraction curves, and differences between the curves are on the order of measurement errors.

[23] Almost as narrow a range of shapes within the memory and erased fraction groups of curves is seen in SIRM results for the hydrothermally produced magnetites (Figure 4c), which have an even wider range of grain sizes (0.8–356 μm). The 0.8, 25, 64, and 94 μm curves are particularly well clustered within either group. The controlling factor for clustering of curves of different grain sizes must be low levels of internal stress because this is the only common factor between Figures 4b and 4c. It cannot be changes in the form, size, or surface roughness of grains resulting from annealing.

[24] TRM memory and erased fraction curves appear in Figure 5 for the four annealed crushed magnetites whose SIRM curves were illustrated in Figure 4b. The coercivity range, aspect, and narrow spread of the TRM erased fraction curves are similar to those of the corresponding SIRM curves. The TRM memory curves, on the other hand, spread quite broadly and have coercivity ranges higher than (1 μm), similar to (9 and 20 μm) or less than (135 μm) those of the SIRM memories in Figure 4b. The Lowrie-Fuller test result is thus of SD-type for the 1 μm grains, neutral for the 9 and 20 μm grains, and MD-type for the 135 μm magnetites. The latter result is remarkable because the 135 μm TRM and SIRM memories both have SD-like inflected decay curves with initial plateaus, the plateau being particularly striking for the TRM memory.

[25] TRM results are rather noisy for the hydrothermal magnetites. Good results were obtained for 20 and 25 μm grains. Their TRM memories are much harder than the corresponding SIRM memory (Figure 4c), a decisively SD-type Lowrie-Fuller test.

[26] Among the annealed crushed magnetites the pattern observed is that SIRM memory decay curves cluster in a group, while the TRM memory decay curves disperse about them in the direction dictated by the Lowrie-Fuller test. Another observation from Figure 5 is that even the hardest TRM memories have more limited initial plateaus, less strongly inflected shapes, and broader coercivity ranges than those of 0.04–0.1 μm SD magnetites.

[27] There is a much better match between SIRM memory decay curves of annealed and hydrothermal magnetites and SIRM decay curves measured for 0.04–0.1 μm SD

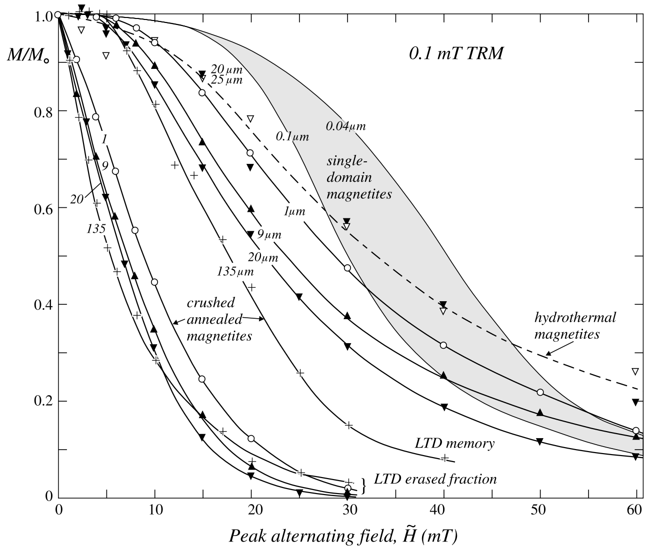

Figure 5. AF demagnetization of weak field TRM for representative crushed annealed and hydrothermal magnetite samples. The erased fraction curves are soft and MD-like, with little size dependence. The LTD memory curves are more size-dependent. They resemble total TRM demagnetization curves of truly SD (0.04 and 0.1 μm) magnetites [*Dunlop*, 1973] but with generally lower coercivities.

grains (Figure 6). The SIRM memory of a 335 μm flux-grown magnetite crystal also demagnetizes within the envelope of the SD curves.

4. Discussion

4.1. Decomposition Into SD-Like and MD-Like Fractions by LTD

[28] When LTD is used as a pretreatment before AF demagnetization, it usually has a minor effect on SD remanence, which in magnetite tends to be inhibited from rotation by magnetostatic effects like shape anisotropy, with magnetocrystalline lattice coupling providing only a minimum switching barrier amounting to 10–15 mT. Domain walls, however, are strongly affected by the precipitous decrease in K_1 between 250 K and T_K = 130 K, the change in sign and momentary vanishing of K_1 at T_K, and the strong increase in anisotropy as the crystal symmetry changes from

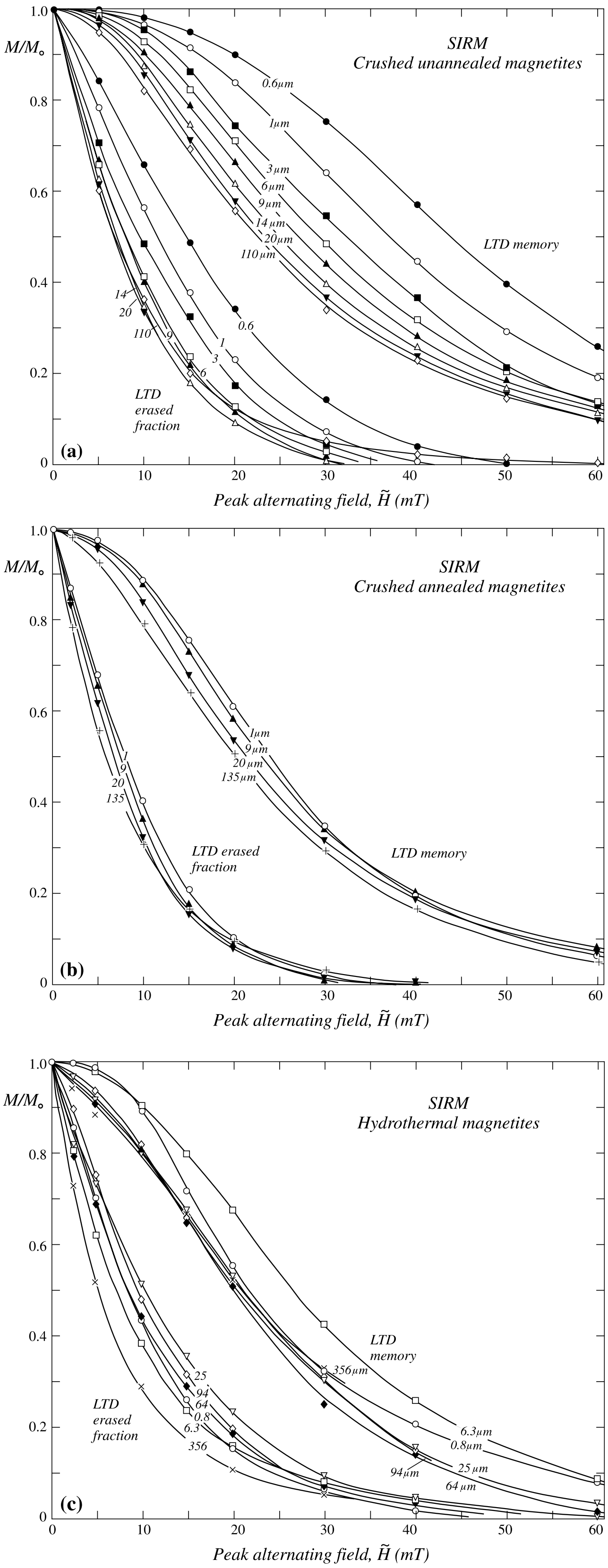

Figure 4. AF demagnetization of SIRM. (a) For the crushed unannealed magnetites the memory remaining after LTD of the SIRM has size-dependent AF curves with inflected SD-like shapes, while the fraction erased by LTD has exponential MD-like AF curves with some grain size dependence. (b) For (selected) crushed annealed magnetite samples the curves are again inflected (SD like) for the memory after LTD and exponential (MD like) for the fraction erased by LTD, but in contrast to Figure 4a, there is little grain size dependence of the curves in either set. (c) For hydrothermal magnetites the LTD memory and erased fraction curves are again SD-like and MD-like in shape, respectively, and relatively grain-size-independent.

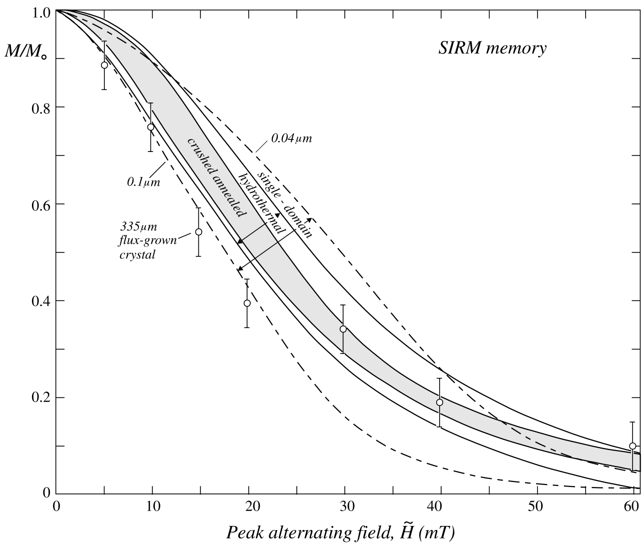

Figure 6. A demonstration that post-LTD SIRM memory AF demagnetization curves for the crushed annealed and hydrothermal magnetite samples lie within the envelope of SIRM demagnetization curves for SD (0.04 and 0.1 μm) magnetites [*Dunlop*, 1973].

cubic to monoclinic at T_V. Two effects come into play. The first is unpinning of domain walls from stress centers and their reequilibration under the influence of the internal self-demagnetizing field H_d. The second is nucleation of domain walls around lattice defects, often at the grain surface [*Heider et al.*, 1988]. The wall nucleus then spreads into the grain (secondary nucleation), again resulting in reequilibration of the positions of other walls. Because H_d has a net demagnetizing effect and LTD is carried out in zero external applied field, the remanence will always decrease after a full cooling-warming cycle.

[29] Before LTD the AF demagnetization curves of our samples are neither strictly SD-like nor MD-like. They are intermediate between these end-members, and their coercivity ranges decrease steadily as the sample grain size increases (Figure 2). LTD reveals that the individual curves are composites with varying proportions of SD-like and MD-like components. For example, for the 1 μm annealed crushed magnetite, LTD removes ~35% of weak field TRM or ARM and ~45% of SIRM, and the memories in each case have SD-like AF demagnetization curves (Figure 3a). The fraction erased has an MD-like AF curve (Figure 4b). This is not too surprising because the size distribution of this sample may extend to truly SD sizes, and we anticipated that LTD would efficiently demagnetize the MD fraction. What is surprising is that even the largest magnetites in this series retain a fraction with apparently SD-like AF behavior. This fraction is 30% of the initial TRM or SIRM for the 135 μm sample (Figure 3b). Although some adhering fine grains may have escaped observation in scanning electron micrographs, a volume of SD material large enough to account for 30% of the remanence is implausible.

[30] The same pattern holds for all three suites of samples, crushed and highly stressed, crushed and stress reduced through annealing, and hydrothermally grown with minimal stress, collectively covering a grain-size range from 0.6 μm to 356 μm. The fraction of remanence erased by LTD has AF decay curves that are soft (with coercivities ≤35 mT, the field at which the memory and pre-LTD demagnetization curves merge; see Figures 3a and 3b) and of MD-like exponential form, even for the finest grains (Figures 4a–4c and 5). The memory fraction remaining after LTD has harder, SD-like AF decay curves (Figures 3–6). Initial plateaus of no demagnetization are best developed for the finer grains, but all curves are distinctly inflected, with inflection points between 20 and 40 mT, usually close to the median destructive field.

[31] How SD-like are the memory curves? For SIRM in the annealed and hydrothermal suites they are very SD-like indeed: The decay curves for all samples fall within the envelope of results for truly SD magnetites (Figure 6). Weak field TRM, on the other hand, demagnetizes over a broader coercivity range than the truly SD magnetites, although the two sets of curves converge around 60 mT (Figure 5).

4.2. Lowrie-Fuller Tests of LTD Memory and Erased Fractions

[32] The contrast between SIRM and TRM behavior translates into contrasting results of the *Lowrie and Fuller* [1971] test for fine- and coarse-grained annealed samples. Figure 7a shows that the TRM memory of the 135 μm grains is at first more resistant to AF cleaning than SIRM memory, but beyond 10 mT (~80% of the remanence) the relative stabilities are reversed, an MD-type Lowrie-Fuller (L-F) test. For fine grains, e.g., 1 μm (Figure 7b), TRM memory is more resistant to AFs than SIRM memory over the entire range of fields, an SD-type L-F test. Intermediate-size PSD grains (9 and 20 μm) have fairly similar TRM and SIRM memory decay curves (Figures 7a and 7b), a transitional/null L-F test result. Although on the basis of AF curve shapes all grain sizes have SD-like memories, the traditional L-F test is still diagnostic of relative size.

[33] Remarkably, the same pattern holds approximately for the LTD erased fractions. The numerical differencing necessary to obtain the erased fraction curves compounds experimental errors, but the 135 μm grains do have SIRM slightly more AF resistant than TRM over the 0–30 mT range, while the 1 μm grains have the opposite trend. Results for the 9 and 20 μm samples are null to MD-like (20 μm, >10 mT). All these decay curves, TRM and SIRM alike, are soft and quasi-exponential in shape.

[34] The AF curves for TRM and SIRM without LTD treatment also obey the Lowrie-Fuller test for the annealed magnetites (e.g., Figures 3a and 3b). This is not so remarkable a result because the shapes of the curves span a range from inflected to quasi-exponential as grain size increases (Figure 2). However, it contrasts with the findings of *Halgedahl* [1998], whose glass-ceramic magnetites all had SD-type Lowrie-Fuller tests for sizes ranging from 0.1 μm to as large as 100 μm.

[35] *Bailey and Dunlop* [1983] proposed that L-F tests of MD and large-PSD (null or crossover) types result from the quasi-exponential shapes of the corresponding AF decay curves. *Xu and Dunlop* [1995] included internal stress as well as curve shape as dual factors determining the L-F test result and were able to reconcile the L-F data of *Heider et al.* [1992] for low-stress magnetites (where the changeover

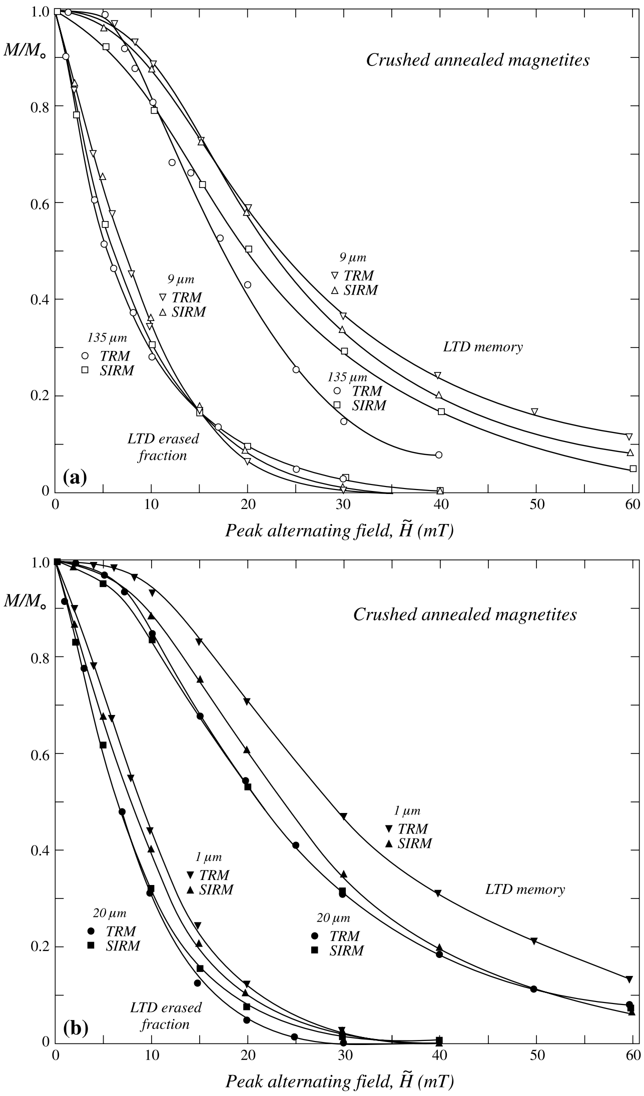

Figure 7. TRM and SIRM demagnetization data from Figures 4b and 5 plotted as Lowrie-Fuller tests. (a) The test result is of MD type (SIRM harder to erase than TRM) for the 135 μm magnetite (above 10 mT for the LTD memory). For the 9 μm magnetite the result is of SD type (TRM harder than SIRM) for the LTD memory and null for the LTD erased fraction. (b) Above 10 mT the test result for the 20 μm magnetite is null for the LTD memory and marginally MD for the LTD erased fraction. For the 1 μm magnetite the result is of SD type for both LTD memory and erased fraction.

from SD-type to MD-type occurs around 100 μm) with other data, such as those of *Johnson et al.* [1975] and *Bailey and Dunlop* [1983], which were interpreted as indicating a "PSD threshold" around 15–20 μm. Our finding complicates matters because curves of basically exponential form seem able to produce SD-type and transitional, as well as MD-type, L-F results.

4.3. Size Dependence of After-LTD Decay Curves: The Effect of Internal Stress

[36] AF demagnetization curves of LTD memory in magnetites crushed from large crystals and separated into narrow size fractions are entirely different depending on whether the grains are untreated or have been annealed after crushing. Unannealed samples have a strong grain size dependence of the AF curves for both the LTD memory and erased fractions of remanence (Figure 4a). In contrast, the SD-like memory and the MD-like erased fractions of annealed samples have nearly identical AF responses for all grain sizes from 0.6 to 135 μm (Figure 4b). The memory response is very similar to that documented by *Dunlop and Argyle* [1991] for small PSD magnetites just above SD size (0.215–0.54 μm) and by *Özdemir and Dunlop* [1998] for millimeter-size natural magnetite crystals. There appears to be a sort of canonical SD behavior revealed by LTD occurring in essentially all grain sizes of magnetite formed in low-stress environments.

[37] Annealing has several possible effects. It heals the lattices of crystal fragments strained by crushing, thereby reducing dislocation densities and internal stress. However, it could also have other physical effects, e.g., reduction of surface roughness (a known factor in magnetite coercivity [*Heider et al.*, 1992]) and particle angularity and overall shape, or chemical effects such as selective oxidation of very fine particles to weakly magnetic hematite or wholesale surface oxidation of grains of all sizes to a cation-deficient magnetite.

[38] We tried to eliminate chemical effects by annealing under vacuum. Some evidence that we were successful comes from largely reversible thermomagnetic curves with minimal indication of hematite and from the fact that coercivities did not increase after annealing, as they would have done for surface-oxidized magnetites. In fact, coercivities of the memory and erased fractions systematically decreased. Comparing Figures 4a and 4b, the after-annealing decay curves of both groups fall just below the lowest curves (110 and 135 μm) of the unannealed magnetites. The reductions in coercivity are quite substantial for the finer grains but are comparatively slight for the largest grains. This could mean that ultrafine particles have been eliminated by oxidation and that this ultrafine "contamination" was largest for the smaller-sized fractions like 0.6 and 1 μm and was negligible for the coarser sizes like 110 and 135 μm.

[39] A more likely explanation is that annealing has reduced internal stress and with it the strength of domain wall pinning by dislocations, i.e., coercivity. Hydrothermal magnetites, which have low stress and are unoxidized, behave in much the same way as annealed magnetites (Figures 4b and 4c). Therefore we attribute the change from grain-size-dependent to size-independent AF behavior to a change from variable high internal stress to a uniform low stress level. There could be also some contribution from the healing of rough, angular, and fractured surfaces. This seems less likely because surface defects and sharp corners are typical sites for domain wall nucleation. Eliminating them would make nucleation more difficult and would increase, not decrease, coercivities.

[40] Whatever the cause of the difference in behavior between unannealed grains and annealed or hydrothermal grains, the observations indicate two types of SD-like moments. One is linked to stress and has size-dependent high AF coercivities of SIRM, about twice as large for 0.6 μm grains as for 110 and 135 μm grains (Figure 4a). The other SD-like source underlies the first and is revealed by

annealing out stress. These moments have SIRM AF demagnetization curves that are only weakly size-dependent and are softer than those of any of the stress-controlled memories (Figure 4b). Hydrothermal magnetites contain only these size-independent moments (Figure 4c). The second type of moment has AF curves that fall between those of 0.04 and 0.1 μm SD grains (Figure 6).

5. What is the Origin of SD-Like Memory?

5.1. Some Basic Constraints

[41] Contaminating ultrafine grains are unlikely to be the source of SD-like memory. There is volumetrically not enough ultrafine material in the larger grain-size samples to explain their high memories (30% of original TRM or SIRM for 135 μm grains). If fines were removed by selective oxidation during annealing, large decreases in coercivity should result, contrary to observations for the 110 and 135 μm samples. In any case, hydrothermal magnetites, which are grown to a uniform size, behave in the same way.

[42] The mechanism of SD-like moments in annealed and hydrothermal magnetites must produce identical AF responses over a size range extending from submicron to at least 350 μm and perhaps as large as a few millimeters. We cannot tailor the SD source to fit the size range; one mechanism must fit all sizes. The additional, size-dependent SD-like source in unannealed grains, most plausibly linked to internal stress, is a separate issue.

5.2. PSD Models and Mechanisms

[43] The earliest PSD model was that of *Verhoogen* [1959], who postulated SD-like behavior of regions of deflected spins surrounding dislocations. The magnitudes of such moments for realistic stress levels were shown by *Shive* [1969] to be too small to explain observed PSD moments. *Stacey* [1962, 1963] proposed two potential PSD sources, Barkhausen discreteness of wall positions and net moments of tapering or other irregularly shaped grains. The latter mechanism has been quantified by *Fabian and Hubert* [1999]. Even grains with regular shapes have net moments if the number of domains is odd [*Dunlop*, 1983; *Xu and Merrill*, 1987]. Imbalance mechanisms of this sort produce significant moments only in small grains with a few domains. They cannot explain memories of 30% in 135 μm magnetite grains, which contain large numbers of domains [*Özdemir and Dunlop*, 1993, 1997; *Özdemir et al.*, 1995].

[44] *Kobayashi and Fuller* [1968] pointed out that with the change in sign of K_1 on passing through T_K, dislocation pileups that act as pinning centers for domain walls on one side of the transition should become centers of repulsion on the other side and vice versa. Given the wholesale reorganization of walls that would ensue, it is difficult to understand how any memory could be recovered in a complete LTD cycle. Obviously, partial recovery does occur, and Kobayashi and Fuller suggested that the moments of regions surrounding in-phase stress centers (their term for pinning centers) would act as PSD sources. Their model is akin to that of *Verhoogen* [1959] but on a larger scale.

[45] *Stacey and Banerjee* [1974] proposed surface moments produced by domain wall terminations as a way of explaining the observed $1/d$ grain size dependence of TRM in magnetite. Although the general occurrence of closure domains in magnetite remains controversial, they are certainly present in large crystals [*Özdemir et al.*, 1995]. Surface moments would then be a result of imbalance of closure domain volumes.

[46] In all these models the PSD moments are inseparable from the body (or surface) domains. Displacements of the walls will modify and ultimately reverse the moments. Nucleation of walls will have a similar effect. Coercivities will therefore be similar to those for wall displacement or nucleation. Furthermore, the magnitudes of moments will be limited by self-demagnetization. These moments have all the attributes of MD magnetization, and there is no reason to expect them to have unusually high coercivities.

[47] *Dunlop* [1977] proposed domain wall moments ("psarks") as a source of SD-like behavior in MD grains. The moment of a domain wall is perpendicular to the domain magnetizations, is unaffected by wall displacement, and can reverse in SD-like fashion without affecting the domain magnetizations. Domain nucleation or destruction adds or subtracts walls and wall moments without affecting psark properties, e.g., coercivity. This coercivity is determined by wall domain reversal and could be high. It is not influenced by self-demagnetizing fields because the two possible states have equal moments. Demagnetizing energy enters only through the barrier to reversal.

[48] There are problems with the model, however. First, only grains with an odd number of walls have net moments, and their percentage contribution to remanence will only be significant in grains with a few walls (1, 3, or 5). Second, reversal of walls may occur by Bloch line propagation rather than coherent rotation, reducing the coercivity. In larger grains, Bloch lines may subdivide the wall in the remanent state, diminishing its moment.

[49] In view of these difficulties the one really satisfactory PSD mechanism, and the only one that is directly demonstrated experimentally, is metastable SD states of MD-size grains [*Halgedahl and Fuller*, 1980, 1983]. Most published observations of metastable SD grains are for pyrrhotite and $x = 0.6$ titanomagnetite, which have critical SD sizes d_0 around 1–2 μm. Magnetite's critical SD volume is 4 orders of magnitude smaller, and it is not clear that even 10 μm grains, let alone 100 or 1000 μm grains, have a significant fraction in metastable SD states. Another problem is that metastable SD grains may nucleate walls in quite small reverse fields. Their coercivities are not necessarily SD-like.

5.3. Mimicking SD Behavior?

[50] A mechanism for generating moments with SD-like AF demagnetization curves of the same form and coercivity range over all magnetite grain sizes remains elusive. One can imagine, however, producing AF curves that mimic SD behavior by isolating a population of domain walls that all have threshold fields ≥10 mT for their displacement. It is also possible that LTD might selectively cause nucleation events below a threshold coercivity: *Boyd et al.* [1984] observed wall nucleation triggered by LTD in metastable SD magnetite. Size-independent exponential demagnetization curves beginning above a threshold field selected by LTD would produce a rough approximation to the memory

demagnetization curves we observe for annealed and hydrothermal magnetites. The observed excellent match to real SD demagnetization curves remains unexplained.

[51] It is not clear that LTD, through wall broadening, would selectively move pinned walls that have a particular range of pinning fields in the absence of wall broadening. It is somewhat easier to imagine LTD triggering nucleation events up to a threshold field. Nucleation is a simple balance between magnetocrystalline forces that bind spins to the lattice and self-demagnetizing fields that favor local reversal of the spins. The $K_1 \rightarrow 0$ response during LTD and the response to AF after LTD are more obviously parallel.

[52] We tentatively hypothesize that nucleation can generate an AF demagnetization curve that mimics SD curves, easy nucleation events triggered by LTD having created an initial plateau up to $\sim$10 mT. The grain-size-independent AF curves of annealed and hydrothermal samples are then easier to understand. Surface sites for nucleation include pits, fractures, corners, and sharp protuberances, which locally lower magnetocrystalline energy. These have the same form and effect in grains of any size, even of millimeter size.

[53] Before-annealing memory demagnetization curves should also be SD look-alikes: They contain the same nucleation-controlled size-independent component as annealed and hydrothermal samples plus an added size-dependent component, which we assume is due to wall unpinning. Nucleation and unpinning must occur simultaneously in these stressed grains, unpinning in the interior and nucleation primarily at the surface. Initial plateaus will result if LTD unpins a selected set of walls having coercivities less than a threshold field, as well as triggering easy nucleation events. The implausible feature of this model is that coercivities due to releasing pinned walls from their stress centers must be larger than coercivities due to nucleating new walls, for 0.6 and 1 μm grains almost twice as large (Figures 4a and 4b). The finer grains are pulverized fragments of large crystals and are indeed likely to have accumulated more stress. Nevertheless, it is hard to imagine how nucleation could be much easier than wall unpinning, an inversion of their usual roles. The very existence of metastable SD grains testifies to the difficulty of nucleating walls.

6. Conclusions

[54] When LTD is used to pretreat weak field remanences like TRM and ARM or strong field SIRM, the resulting memory has inflected AF demagnetization curves with initial plateaus resembling those of SD grains, while the fraction erased by LTD has exponential MD-like curves. This clear separation into MD and SD-like fractions holds true even for magnetite grains as large as 350 μm, with volumes $>10^{10}$ times the critical SD volume. In unannealed grains crushed from large crystals, the AF demagnetization curves of both memory and erased fractions are grain-size-dependent, larger grains being softer. In low-stress annealed grains and hydrothermally produced magnetites the AF demagnetization curves of both fractions are almost size-independent for SIRM memory and are weakly size-dependent for TRM memory.

[55] Adhering fine particles cannot explain the magnitude of the SD-like memory (30% of TRM or SIRM in 135 μm grains). Published PSD mechanisms, such as dislocation-line moments, imbalance moments due to irregular shape and other causes, surface moments, domain wall moments, and metastable SD grains also fail to explain the observations over such a broad size range. We therefore propose an ad hoc model by which the post-LTD coercivity spectrum of wall nucleation events mimics the size-independent SD-like behavior of memory in low-stress magnetites, and the coercivity spectrum resulting from releasing strongly pinned walls in highly stressed grains explains the additional high-coercivity fraction of memory in unannealed grains.

[56] We observe that the *Lowrie and Fuller* [1971] test correctly classifies the grain sizes/domain states of the memory and erased fractions of annealed grains (Figures 7a and 7b). The TRM and SIRM demagnetization curves of memory fractions have inflected SD-like shapes for all grain sizes, while the erased fraction curves are exponential and MD-like. Nevertheless, the relative TRM and SIRM stabilities are SD-type for the 1 μm grains, mainly null or transitional for the 9 and 20 μm grains, and MD-type for the 135 μm grains. This behavior confounds the theory that the Lowrie-Fuller test works because of demagnetization curve shape but makes the test more powerful than anticipated.

[57] **Acknowledgments.** For very positive reviews and suggestions we are grateful to Mike Fuller, Randy Enkin, and an anonymous reviewer. Kappa bridge and low-temperature SIRM warming experiments were carried out at the Institute for Rock Magnetism, which is operated with support from the Earth Sciences Division of the National Science Foundation, the Keck Foundation, and the University of Minnesota. The University of Toronto rock magnetism research program is supported by the Natural Sciences and Engineering Research Council of Canada through grant A7709 to D.J.D.

References

Bailey, M. E., and D. J. Dunlop (1983), Alternating field characteristics of pseudo-single-domain (2–14 μm) and multidomain magnetite, *Earth Planet. Sci. Lett.*, *63*, 335–352.

Boyd, J. R., M. Fuller, and S. Halgedahl (1984), Domain wall nucleation as a controlling factor in the behaviour of fine magnetic particles in rocks, *Geophys. Res. Lett.*, *11*, 193–196.

Day, R., M. D. Fuller, and V. A. Schmidt (1977), Hysteresis properties of titanomagnetites: Grain size and composition dependence, *Phys. Earth Planet. Inter.*, *13*, 260–267.

Dunlop, D. J. (1973), Thermoremanent magnetization in submicroscopic magnetite, *J. Geophys. Res.*, *78*, 7602–7613.

Dunlop, D. J. (1977), The hunting of the 'psark', *J. Geomagn. Geoelectr.*, *29*, 293–318.

Dunlop, D. J. (1983), The demagnetizing energy and demagnetizing factor of a multidomain ferromagnetic cube, *Geophys. Res. Lett.*, *10*, 79–82.

Dunlop, D. J., and K. S. Argyle (1991), Separating multidomain and single-domain-like remanences in pseudo-single-domain magnetites (215–540 nm) by low-temperature demagnetization, *J. Geophys. Res.*, *96*, 2007–2017.

Dunlop, D. J., and K. S. Argyle (1997), Thermoremanence, anhysteretic remanence and susceptibility of submicron magnetites: Nonlinear field dependence and variation with grain size, *J. Geophys. Res.*, *102*, 20,199–20,210.

Dunlop, D. J., and Ö. Özdemir (1997), *Rock Magnetism: Fundamentals and Frontiers*, 573 pp., Cambridge Univ. Press, New York.

Dunlop, D. J., Ö. Özdemir, and P. W. Schmidt (1997), Paleomagnetism and paleothermometry of the Sydney Basin: 2. Origin of anomalously high unblocking temperatures, *J. Geophys. Res.*, *102*, 27,285–27,295.

Enkin, R. J., and W. Williams (1994), Three-dimensional micromagnetic analysis of stability in fine magnetic grains, *J. Geophys. Res.*, *99*, 611–618.

Fabian, K., and A. Hubert (1999), Shape-induced pseudo-single-domain remanence, *Geophys. J. Int.*, *138*, 717–726.

Halgedahl, S. L. (1998), Revisiting the Lowrie-Fuller test: Alternating field demagnetization characteristics of single-domain through multidomain glass-ceramic magnetite, *Earth Planet. Sci. Lett.*, *160*, 257–271.

Halgedahl, S. L., and M. Fuller (1980), Magnetic domain observations of domain nucleation processes in fine particles of intermediate titanomagnetite, *Nature*, *288*, 70–72.

Halgedahl, S. L., and M. Fuller (1983), The dependence of magnetic domain structure upon magnetization state with emphasis on nucleation as a mechanism for pseudo-single-domain behavior, *J. Geophys. Res.*, *88*, 6505–6522.

Heider, F., and L. T. Bryndzia (1987), Hydrothermal growth of magnetite crystals (1 μm to 1 mm), *J. Crystal Growth*, *84*, 50–56.

Heider, F., D. J. Dunlop, and N. Sugiura (1987), Magnetic properties of hydrothermally recrystallized magnetite crystals, *Science*, *236*, 1287–1290.

Heider, F., S. L. Halgedahl, and D. J. Dunlop (1988), Temperature dependence of magnetic domains in magnetite crystals, *Geophys. Res. Lett.*, *15*, 499–502.

Heider, F., D. J. Dunlop, and H. C. Soffel (1992), Low-temperature and alternating field demagnetization of saturation remanence and thermoremanence in magnetite grains (0.037 μm to 5 mm), *J. Geophys. Res.*, *97*, 9371–9381.

Johnson, H. P., W. Lowrie, and D. V. Kent (1975), Stability of anhysteretic remanent magnetization in fine and coarse magnetite and maghemite particles, *Geophys. J. R. Astron. Soc.*, *41*, 1–10.

Kobayashi, K., and M. Fuller (1968), Stable remanence and memory of multi-domain materials with special reference to magnetite, *Philos. Mag.*, *18*, 601–624.

Lowrie, W., and M. Fuller (1971), On the alternating field demagnetization characteristics of multidomain thermoremanent magnetization in magnetite, *J. Geophys. Res.*, *76*, 6339–6349.

McClelland, E., and V. P. Shcherbakov (1995), Metastability of domain state in multidomain magnetite: Consequences for remanence acquisition, *J. Geophys. Res.*, *100*, 3841–3857.

McClelland, E., A. R. Muxworthy, and R. M. Thomas (1996), Magnetic properties of the stable fraction of remanence in large multidomain (MD) magnetite grains: Single-domain or MD?, *Geophys. Res. Lett.*, *23*, 2831–2834.

Merrill, R. T. (1970), Low-temperature treatment of magnetite and magnetite-bearing rocks, *J. Geophys. Res.*, *75*, 3343–3349.

Moon, T. S., and R. T. Merrill (1984), The magnetic moments of non-uniformly magnetized grains, *Phys. Earth Planet. Inter.*, *34*, 186–194.

Moon, T. S., and R. T. Merrill (1985), Nucleation theory and domain states in multidomain magnetic material, *Phys. Earth Planet. Inter.*, *37*, 214–222.

Muxworthy, A. R., and E. McClelland (2000), The causes of low-temperature demagnetization of remanence in multidomain magnetite, *Geophys. J. Int.*, *140*, 115–131.

Newell, A. J., and R. T. Merrill (1999), Single-domain critical sizes for coercivity and remanence, *J. Geophys. Res.*, *104*, 617–628.

Özdemir, Ö., and D. J. Dunlop (1993), Magnetic domain structures on a natural single crystal of magnetite, *Geophys. Res. Lett.*, *20*, 1835–1838.

Özdemir, Ö., and D. J. Dunlop (1997), Effect of crystal defects and internal stress on the domain structure and properties of magnetite, *J. Geophys. Res.*, *102*, 20,211–20,224.

Özdemir, Ö., and D. J. Dunlop (1998), Single-domain-like behavior in a 3-mm natural single crystal of magnetite, *J. Geophys. Res.*, *103*, 2549–2562.

Özdemir, Ö., S. Xu, and D. J. Dunlop (1995), Closure domains in magnetite, *J. Geophys. Res.*, *100*, 2193–2209.

Parry, L. G. (1965), Magnetic properties of dispersed magnetite powders, *Philos. Mag.*, *11*, 303–312.

Shive, P. N. (1969), Dislocation control of magnetism, *J. Geomagn. Geoelectr.*, *21*, 519–529.

Stacey, F. D. (1962), A generalized theory of thermoremanence, covering the transition from single-domain to multi-domain magnetic grains, *Philos. Mag.*, *7*, 1887–1900.

Stacey, F. D. (1963), The physical theory of rock magnetism, *Adv. Phys.*, *12*, 45–133.

Stacey, F. D., and S. K. Banerjee (1974), *The Physical Principles of Rock Magnetism*, 195 pp., Elsevier, New York.

Verhoogen, J. (1959), The origin of thermoremanent magnetization, *J. Geophys. Res.*, *64*, 2441–2449.

Williams, W., and D. J. Dunlop (1995), Simulation of magnetic hysteresis in pseudo-single-domain grains of magnetite, *J. Geophys. Res.*, *100*, 3859–3871.

Xu, S., and D. J. Dunlop (1993), Theory of alternating field demagnetization of multidomain grains and implications for the origin of pseudo-single-domain remanence, *J. Geophys. Res.*, *98*, 4183–4190.

Xu, S., and D. J. Dunlop (1995), Toward a better understanding of the Lowrie-Fuller test, *J. Geophys. Res.*, *100*, 22,533–22,542.

Xu, S., and R. T. Merrill (1987), The demagnetizing factors in multidomain grains, *J. Geophys. Res.*, *92*, 10,657–10,665.

Xu, S., and R. T. Merrill (1989), Microstress and microcoercivity in multidomain grains, *J. Geophys. Res.*, *94*, 10,627–10,636.

D. J. Dunlop, Geophysics, Physics Department, University of Toronto, Toronto, Ontario, Canada M5S 1A7. (dunlop@physics.utoronto.ca)

F. Heider, Physical Failure Analysis, Infineon Technologies, Siemensstr. 2, 9500 Villach, Austria. (franz.heider@infineon.com)

S. Xu, JDL Digital Systems, 1033 Andover Park East, Seattle, WA 98188, USA. (derek@jdlds.com)